European Union's Seventh Framework Programme
Grant Agreement Nº: 603521

Project Acronym: **PREFACE**

Project full title: **Enhancing prediction of tropical Atlantic climate and its impacts**

Instrument: Collaborative Project

Theme: ENV.2013.6.1-1 – *Climate-related ocean processes and combined impacts of multiple stressors on the marine environment*

Start date of project: 1 November 2013 Duration: 48 Months

Deliverable Reference Number and Title:

D 7.1

"Assessment on the representation of s2d TAV by current model configurations"

Lead work package[1] for this deliverable: WP7

Lead contractor[1] for this deliverable: CERFACS

Due date of deliverable: 31/10/2015

Actual submission date:

Project co-funded by the European Commission within the Seven Framework Programme (2007-2013)		
Dissemination Level		
PU	Public	PU
PP	Restricted to other programme participants (including the Commission Services)	
RE	Restricted to a group specified by the Consortium (including the Commission Services)	
CO	Confidential, only for members of the Consortium (including the Commission Services)	

[1] Name of beneficiary (=institute/organisation/university)

Contribution to project objectives – with this deliverable, the project has contributed to the achievement of the following objectives (see Annex I / DOW, Section B1.1.):

N.º	Objective	Yes	No
1	Reduce uncertainties in our knowledge of the functioning of Tropical Atlantic (TA) climate, particularly climate-related ocean processes (including stratification) and dynamics, coupled ocean, atmosphere, and land interactions; and internal and externally forced climate variability.	X	
2	Better understand the impact of model systematic error and its reduction on seasonal-to-decadal climate predictions and on climate change projections.	X	
3	Improve the simulation and prediction TA climate on seasonal and longer time scales, and contribute to better quantification of climate change impacts in the region.	X	
4	Improve understanding of the cumulative effects of the multiple stressors of climate variability, greenhouse-gas induced climate change (including warming and deoxygenation), and fisheries on marine ecosystems, functional diversity, and ecosystem services (e.g., fisheries) in the TA.		X
5	Assess the socio-economic vulnerabilities and evaluate the resilience of the welfare of West African fishing communities to climate-driven ecosystem shifts and global markets.		X

Authors of this deliverable:

E. Sanchez-Gomez, *CERFACS, Toulouse, France*

List of beneficiaries

No	Name	Short Name
1	UNIVERSITETET I BERGEN	UiB
3	CENTRE EUROPEEN DE RECHERCHE ET DE FORMATION AVANCEE EN CALCUL SCIENTIFIQUE	CERFACS
5	METEO-FRANCE	MF-CNRM
7	HELMHOLTZ ZENTRUM FUR OZEANFORSCHUNG KIEL	GEOMAR
12	WAGENINGEN UNIVERSITY	WU
15	FUNDACIO INSTITUT CATALA DE CIENCIES DEL CLIMA	IC3
16	UNIVERSIDAD COMPLUTENSE DE MADRID	UCM
27	UNIVERSITY OF NIGERIA	UNN

Deviation from planned efforts for this deliverable:

(PLEASE ONLY COMMENT IF THERE WERE DEVIATIONS FROM THE ORIGINAL PLAN[2] IN PERSON-MONTHS PER BENEFICIARY[1] AND/OR WORK PACKAGE OR OTHER RESOURCE USE FOR ACHIEVEMENT OF THIS DELIVERABLE)

There has been a minor deviation from the original plan for beneficiary WU (12). Originally all 24 PMs for this beneficiary were devoted to D7.2 (scheduled for month 36). However, WU has conducted some research in the framework of task 7.1, by the analysis of the Bjerknes feedback in CMIP5 simulations, that it is necessary to understand how climate models represent the equatorial Atlantic variability. This was not explicitly mentioned in the DOW, but this analysis will help to design and develop model modifications in task 7.2. The beneficiary WU (12) devoted approximately 6 PMs to this key issue. We estimate that the work engaged by WU for D7.2 will be addressed with the remaining 18 PMs of their total contribution to WP7.

Report on the deliverable:

(SHORT DESCRIPTION OF WORK PERFORMED; MAIN RESULTS ACHIEVED; CONTRIBUTION TO WP OBJECTIVES and TASKS)

D7.1: Report on the assessment of the representation of seasonal to decadal tropical Atlantic variability by the state-of-the-art coupled models and its relation to mean state errors based not only on existing simulations (CMIP5 and SPECS), but also on new PREFACE models configurations.

This deliverable contributes to the following WP objectives:

1. To make an assessment of the representation of Tropical Atlantic variability at s2d timescales by the state-of-the-art climate models (CMIP5 and other specific configurations).
2. To understand through statistical analysis and model experimentation the relationship between the model systematic error and the representation of Tropical Atlantic variability at s2d timescales.

[2] See List of person-months, nature and dissemination level of deliverable

1. Representation of Tropical Atlantic modes of variability by CMIP5 models

E. Exarchou[1], I. Polo[2], B. Rodriguez-Fonseca[2], E. Sanchez-Gomez[3]
[1] IC3, Barcelone, Spain
[2] UCM, Madrid, Spain
[3] CERFACS, Toulouse, France

Tropical Atlantic variability (TAV) features two dominant modes with distinct spatial patterns of Sea Surface Temperature (SSTs): the first one is an inter-hemispheric meridional SST gradient associated to cross-equatorial surface winds, also called the Atlantic Meridional Mode (AMM) (Carton et al 1996, Chang et al 1997, Servain et al. 1999, Ruiz-Barradas et al 2000, Chiang and Vimont 2004). The second mode is characterized by a zonal SSTs gradient over the equatorial area, and it is known as the Equatorial Mode (EM hereinafter), Zonal Mode or Atlantic Niño (Carton et al 1996, Xie and Carton 2004, Chang et al 2006; Huang and Shukla 2005, Keenlyside and Latif 2007). The seasonality of the AMM and EM is different, while AMM peaks in boreal spring; the EM does later in boreal summer. The AMM is the dominant mode of variability at decadal timescales, though decadal peaks have also identified in the EQ from observations (Nnamchi et al. submitted).

The representation of the EM by state-of-the-art coupled models was investigated by Richter et al. 2014 using the pre-industrial (piControl) experiments from CMIP5 (Coupled Model Intercomparison Phase 5, Taylor et al. 2012) data base. They show, that in despite of the persistent biases present in the mean climate, most of models are able to reproduce observed equatorial variability in terms of spatial structure and explained variance. Here we have extended this analysis to other variability modes, and also applying other approaches.

1.1 The Equatorial Modes

To analyse Tropical Atlantic variability to seasonal from decadal timescales, we have used an Empirical Orthogonal Function (EOFs) analysis of the monthly SST anomalies for both piControl experiments from 17 CMIP5 models (see Table 1) and the HadISST observations (Rayner et al. 2003). The resulting EOFs have been analysed, focusing on the spatial structure and on the seasonal cycle of the modes obtained.

Results show that in general CMIP5 models seem to represent correctly the first 3 modes of variability over the Tropical Atlantic. In the observations, the first and third modes correspond to equatorial Atlantic variability, whereas the second mode consists of a meridional SST dipole (not shown), corresponding to the AMM. In the following, we focus on equatorial Atlantic variability, then on modes 1 and 3. The first mode is known as the equatorial basin-wide mode (Martin-Rey et al. 2015) and the third mode as the South Atlantic ocean dipole (SAOD, Nnamchi et al. 2011).

Most of the models also simulate these 2 modes in the same order of explained variance as the observations. Figures 1 (top panel) shows the Taylor diagrams in terms of pattern correlation and mean error for both equatorial modes (mode 1 and mode 3). In general models capture well the spatial structure of the equatorial modes. In particular, models represent better the mode 3. However the seasonality of the modes (Figure 1, low panel) differs from the observations especially for the basin-wide mode. In the observations this mode peaks in boreal summer while for models is more active in boreal autumn-winter. The SAOD mode peaks in boreal summer for most of the models and the observations.

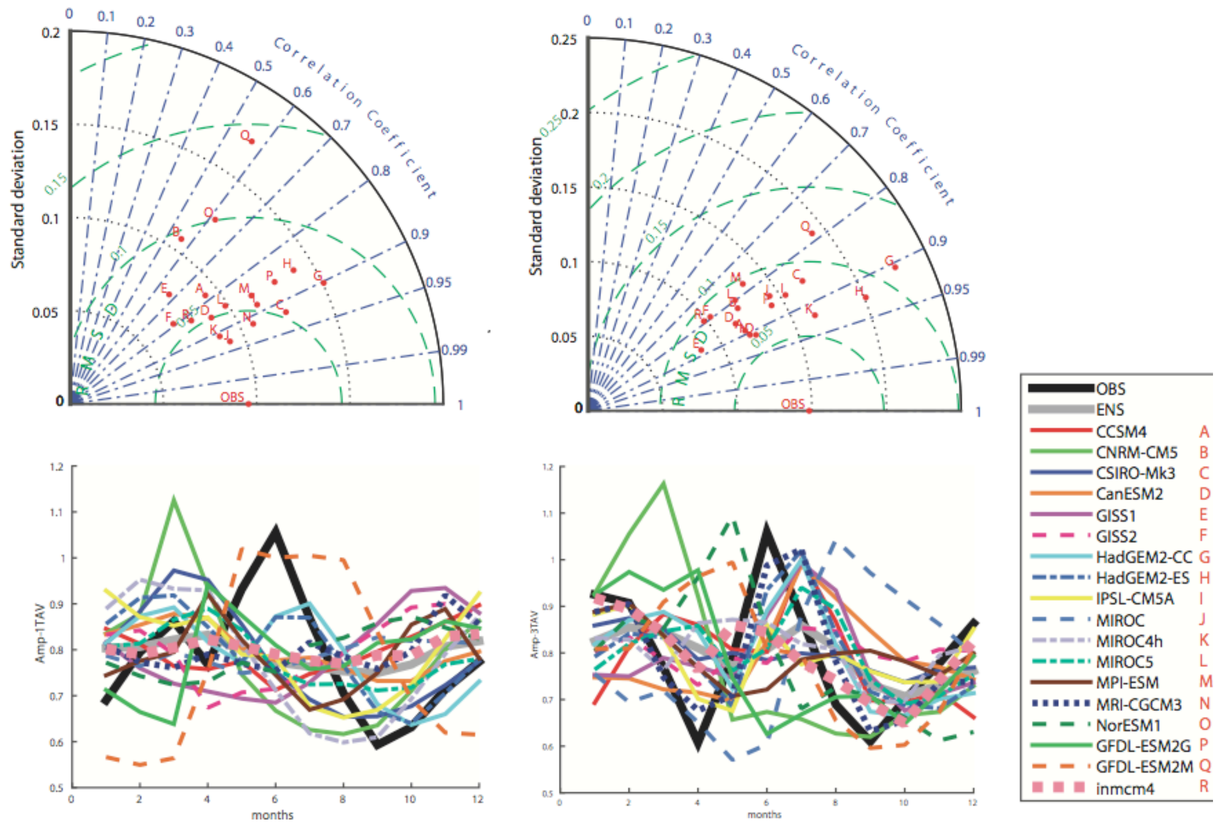

Figure 1. *Top: Taylor diagram of the 18 models from CMIP5 piControl (see table 1) for mode 1 (left, basin-wide mode) and mode 3 (right, SAOD). Bottom: Seasonal cycle of the mode 1 (left) and mode 3 (right).*

This suggests that the models simulate better the autumn-winter equatorial Atlantic variability; nevertheless some variability is also present in boreal summer.

The performance of the modes in the in relation to the mean global bias is discussed in the deliverable 8.1.

Modeling Center (or Group)	Institute ID	Model Name	Nyears/ Resolution
Canadian Centre for Climate Modelling and Analysis	CCCMA	CanESM2	996/128x64
National Center for Atmospheric Research	NCAR	CCSM4	501/288x192
Centre National de Recherches Meteorologiques / Centre Europeen de Recherche et Formation Avancees en Calcul Scientifique	CNRM-CERFACS	CNRM-CM5	850/256 x 128
Commonwealth Scientific and Industrial Research Organization in collaboration with Queensland Climate Change Centre of Excellence	CSIRO-QCCCE	CSIRO-Mk3.6.0	500/192x96
NOAA Geophysical Fluid Dynamics Laboratory	NOAA GFDL	GFDL-ESM2G GFDL-ESM2M	500/ 500
NASA Goddard Institute for Space Studies	NASA GISS	GISS-E2-H GISS-E2-R	531/144x90 550/144x90
Met Office Hadley Centre	MOHC	HadGEM2-CC HadGEM2-ES	240/192x145 575/
Institute for Numerical Mathematics	INM	INM-CM4	500/180x120
Institut Pierre-Simon Laplace	IPSL	IPSL-CM5A-LR	1000/96x96
Japan Agency for Marine-Earth Science and Technology, Atmosphere and Ocean Research Institute (The University of Tokyo), and National Institute for Environmental Studies	MIROC	MIROC-ESM-CHEM	255/128x64
Atmosphere and Ocean Research Institute (The University of Tokyo), National Institute for Environmental Studies, and Japan Agency for Marine-Earth Science and Technology	MIROC	MIROC4h MIROC5	100/640x320 670/256x128
Max Planck Institute for Meteorology	MPI-M	MPI-ESM-LR	1000/192x96
Meteorological Research Institute	MRI	MRI-CGCM3	500/320x160
Norwegian Climate Centre	NCC	NorESM1-M	501/144x96
Met Office Hadley Centre	MOHC	OBS-HadISST	145/360x180

Table1: Models from CMIP5 experiments used in this analysis and observational dataset.

1.2 The Atlantic Meridional Mode

In this work we have investigated the representation of the AMM by the CMIP5 models. Two complementary approaches have been developed in PREFACE: i) The first one analyses the CMIP5 multi-model ensemble; ii) and the second one uses the innovative technique of Partial Linear Squares (PLS) regression to identify modes of variability in models and reanalysis.

I) The Atlantic Meridional Mode in CMIP5

In this case, we have used the historical experiments in order to compare more properly to the observations. The period of the analysis is 1950-2005. The AMM in models is compare to the one obtained from two different reanalysis: NCEP/NCAR (Kalnay et al. 1996) and Twenty Century reanalysis (20CR, Compo et al. 2011). To compute the AMM we have followed the methodology described in Chiang and Vimont, 2004, which is based on a Maximum Covariance Analysis (MCA) between the SSTs and 10 m winds (two components) fields. The analysis is performed by each season separately, considering as JFM (winter), AMJ (spring), JAS (summer) and OND (autumn). In order to remove climate trends, the data, for both models and observations, are previously detrended using the least-squares technique. All the models have been interpolated to the same common grid 1.5^{o} x 1.5^{o} for comparability.

A preliminary analysis reveals that the AMM spatial structure and percentage of covariance explained can be different amongst the members of one model. This indicates that internal variability is very important in the processes governing the AMM. For this reason, in this analysis we have included only models with 3 members or more in the CMIP5 historical experiments. This leads to an ensemble of 17 models. In order to increase the statistical robustness, the 3 members have been concatenated before computing MCA.

Figure 2 shows the zonal means of SST and two wind components (U and V) corresponding to the anomalies associated to the AMM for models and reanalysis. The models are represented by the ensembles mean (red line) and inter-models spread (gray shading) calculated as one standard deviation.

We show only JFM and AMJ seasons, when the AMM is most active during the year. From figure 2a-b it can be noticed that the intermodal spread is larger in the southern hemisphere, reaching until 0.3-0.4^{o}C. In winter, both reanalysis are in the spread of models, however this is not the case of spring season. Models underestimate clearly the strength of the SST meridional gradient, with anomalies in SST much lower in the southern hemisphere comparing to reanalysis. This indicates that the SST dipole is not present in all models of the ensemble.

Concerning surface wind anomalies, the spatial structure of zonal winds (figure 2c-d) is correctly simulated in models, however only northern hemisphere anomalies are slightly underestimated in JFM and overestimate in AMJ, which is coherent with the weaker SSTs anomalies in the southern hemisphere. Meridional winds anomalies are also correctly simulated, however the latitudinal position of the maximum cross-equatorial wind is located southwards in models (figure 2e-f). This is connected to a too southward location of the Inter-Tropical Convergence Zone, which is a common model bias (Richter et al. 2008, 2012).

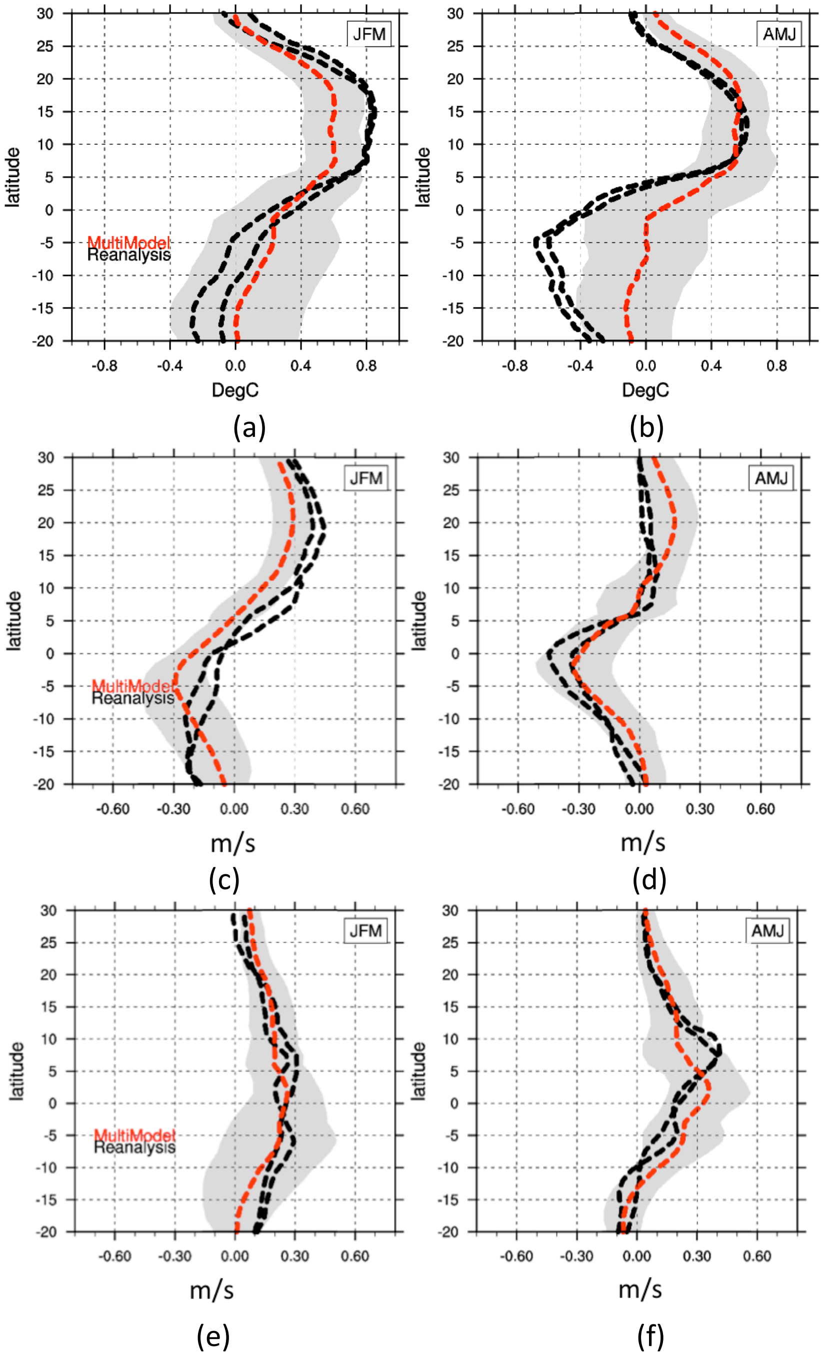

Figure 2: *Zonal means of SST (a-b), zonal (c-d) and meridional (e-f) 10m winds anomalies associated to the AMM in models and reanalysis (black dashed lines). The models are represented by the ensemble mean (red line) and the inter-model spread (gray shading) computed from one standard deviation.*

To conclude, the ensemble of CMIP5 models considered in this work represent the AMM, though the strength of the inter-hemispheric gradient is clearly underestimated, whereas winds structures are correctly simulated. It is difficult to determine a link between the errors in models mean climate and the representation of the AMM, since mean state biases are very similar amongst the models. Figure 3 shows the main common errors found in coupled models in the Tropical Atlantic: the warm bias SSTs in the south-eastern part of the basin; the too southward location of the ITCZ, in particular from winter to spring; and the weaker surface wind speed in the south Atlantic.

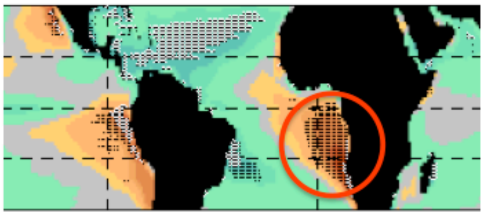

Warm SST bias in the southeast Tropical Atlantic (from Toniazzo and Woolnough, 2013)

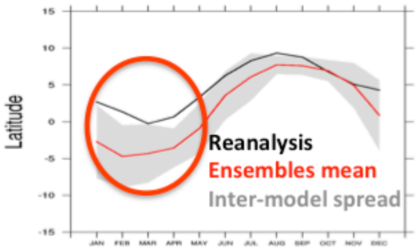

Seasonal cycle of the ITCZ location

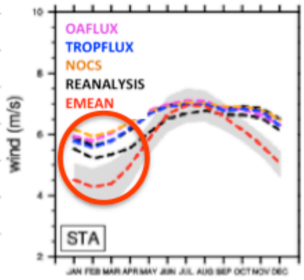

Seasonal cycle of the surface wind speed in the South Atlantic

Figure 3: *Left : SST bias in CMIP5 models from Toniazzo and Woolnough 2013, hatching indicates where most of model agree in the sign of the bias. Center: Sesasonal cycle of the latitudinal position of the ITCZ computed as the maximum precipitation. The 20CR reanalysis is represented by the black line, the models ensembles mean by the red line and the inter-model spread by the gray shading. Right: Seasonal cycle of the surface wind speed bias in the south Tropical Atlantic, compared with different products: 20CR, OAFLUX, NOCS and TROPFLUX datasets. The models ensemble mean is represented by the red line and the inter-model spread by the gray shading*

Warmer SSTs anomalies in the southeast Tropical Atlantic comparing to the northern part of the basin can inhibit the anomalous cooling and the formation of an inter-hemispheric SST gradient. At the same time a too southward ITCZ leads to a weaker wind speed bias in the southern hemisphere, though wind speed in the northern hemisphere is correctly simulated (not shown) by models. This indicates a north-south bias in the wind strength, which decreases the rate of SST cooling (or warming for the negative phase) by latent heat loss in the southern hemisphere comparing to the northern hemisphere.

II) PLS technique applied to AMM

The Partial Least Squares (PLS) methodology is a regression methodology that is used in order to analyze a set of response variables Y in terms of a set of predictors X. It combines features from multiple linear regression and PCA. PLS creates mutually orthogonal components that maximize the covariance between the dependent and independent variables. PLS is a fairly novel approach in identifying teleconnection patterns. It has been recently demonstrated that the PLS regression can successfully extract consistent teleconnection patterns across different models and thus can be a useful methodology to evaluate models in terms of their ability to reproduce leading teleconnection patterns, such as the North Atlantic Oscillation and the East Atlantic pattern (Gonzalez-Reviriego et al., 2014). Here, we apply the PLS regression method in order to identify the AMM, one of the leading mode of variability in the Tropical Atlantic. We have focused on spring season (April-June), where the AMM peaks. Two sets of model data have been considered from the simulations performed with EC-Earth2.3 under the CMIP5 framework: one set consists in decadal predictions initialized from observational data every 1st November from 1993 to

2009, and the second set is a historical simulation (see Table 2). The set of response variables Y we use are the teleconnection patterns for the variables SST, zonal surface wind U and meridional surface wind V for the months AMJ, when this mode is more active, for the period 1960-2005. The teleconnection patterns are obtained with joint singular value decomposition (SVD) method from NCEP reanalysis data, and they are provided by CERFACS. The set of predictors X is the model time series of SST, U and V anomaly fields for the corresponding months and years.

Exp ID	Resolution	Ensembles	Initialized	Period
Init	ORCA1L46-T255L91	5	Every year, 1st November, 10 years long	1960-2005
Histo	ORCA1L46-T255L91	3	Once in 1960 from piControl	1960-2005

Table 2: *Summary of experiments used in this study.*

We find that even though the AMM spatial patterns in SST, U and V can be extracted from both initialized and historical sets of experiments during AMJ (figure 4, spatial patterns for SST), only in the initialized experiment Init the AMM is a leading mode of variability, explaining more than 60% of the response variables (figure 5). The low explained variance in Histo is likely because of averaging out different ensemble members in which the variability is not in phase. Furthermore, we find that the explained variance does not significantly change as a function of forecast time in Init (figure 5). In both Init and Histo the explained variance is less than the one obtained when the PLS methodology is applied directly to the NCEP SST, U and V time series in order to predict the NCEP spatial patterns (figure 5).

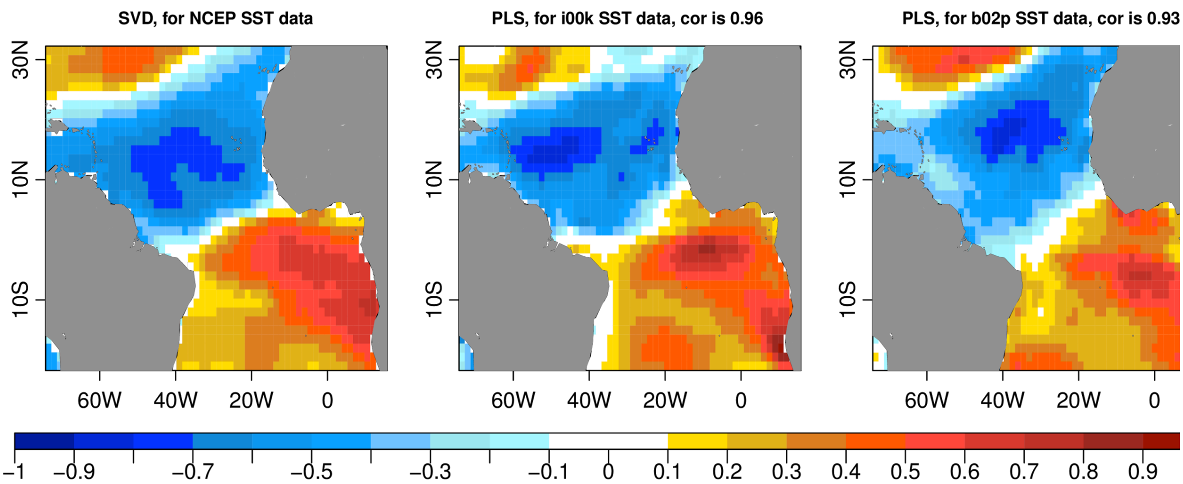

Figure 4: *Spatial structure of the SST pattern in AMM (months AMJ) for the period 1960-2005. Left: obtained with the SVD methodology from the NCEP reanalysis data (provided by CERFACS). Middle and right: obtained with the PLS methodology, where we used model SSTs as predictors in order to predict the NCEP SST pattern (left), using data from the the initialized experiment (Init, middle plot) for the first forecast year, and from the historical experiment (Histo, right plot). The spatial correlation between the model and the NCEP spatial structures is 0.96 for init and 0.93 for Hist.*

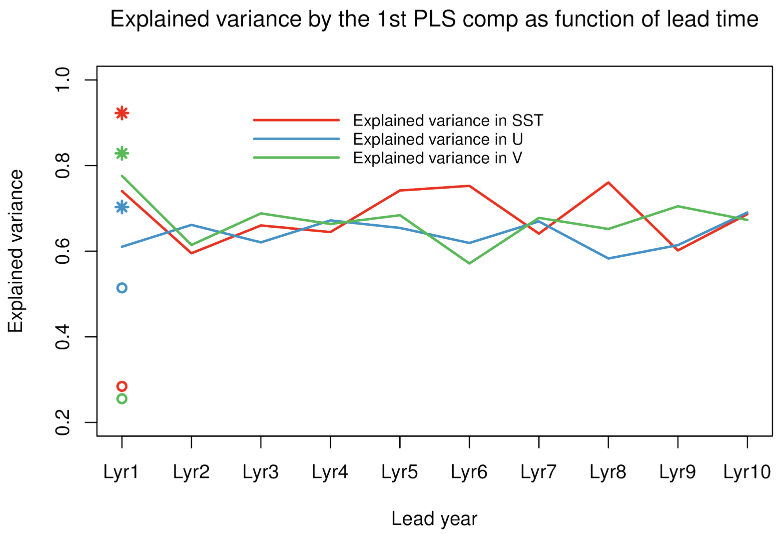

Figure 5: *Explained variance by the first PLS component in predicting the AMM patterns (months AMJ) for the period 1960-2005, in SST (red), U (blue) and V (green), as a function of forecast time (in years). Lines: the explained variance for the initialized run Init. The asterisks show the explained variance in the corresponding variables when the PLS method is applied in the NCEP data. The circles denote the explained variance in the historical run Histo. For illustration purposes the points are located in Ly1, but they are not a function of the forecast time.*

Our future work is to extend this methodology to other CMIP5 models (Init and Histo) and also to include the EM in our analysis.

2. Representation of the mechanisms for seasonal to decadal variability: feedbacks and role of the thermodynamic processes and ocean dynamics

AL Deppenmeier[1], R. Haarsma[1], N. Keenlyside[2], M. Latif[3], H. Nnamchi[4], Y. Planton[5], E. Sanchez-Gomez[6], A. Voldoire[5]

[1] WU, Wageningen, Netherlands

[2] UiB, Bergen, Norway

[3] GEOMAR, Kiel, Germany

[4] UNN, Nsukka, Nigeria

[5] MF-CNRM, Toulouse, France

[6] CERFACS, Toulouse, France

The tropical coupled ocean-atmosphere variability contains two major feedback mechanisms: The Bjerknes feedback (Ruiz-Barradas et al. 2000, Keenlyside and Latif 2007, Janssen et al. 2008), BF hereinafter and the Wind-Evaporation-SST feedback (WES) (Xie and Philander 1994, Xie and Carton 2004, Chang et al. 1997). Both mechanism have been largely studied from theoretical models, observations, reanalysis and coupled models. The BF feedback is responsible of the equatorial Atlantic variability (EM), and the WES feedback is a thermodynamic air-sea interaction that creates and maintains the meridional SST gradients.
The representation of these mechanisms by state-of-the-art models (CMIP5) has been investigated here.

We have conducted further analysis in order to improve our understanding of the role of thermodynamics versus the ocean dynamics in generating SSTs variability in the Tropical Atlantic (2.3).

2.1 The Bjerknes feedback in CMIP5 models

(Deppenmeier et al. 2015, under revision)

Several studies have already investigated this feedback in general circulation models (GCMs) (Dewitt et al. 2005, Ding et al., 2015, Munoz et al. 2014). The present work has analysed the BF in reanalysis data (ERA-Interim (ERAI), Dee et al. 2011) for the atmosphere and ORAS4 (Balmaseda et al. 2013) for the ocean) and in 36 CMIP5 models. The Bjerknes feedback consists of three parts: the influence of eastern equatorial SST anomalies on zonal wind stress (τ_u) anomalies in the western basin, $\lambda_{SST\rightarrow\tau}$; the wind stress anomaly influence on the eastern equatorial heat content (HC) anomalies $\lambda_{\tau\rightarrow HC}$; and the local response of SST to changes in HC, $\lambda_{HC\rightarrow SST}$ (Keenlyside and Latif 2007).

In order to understand the mechanism of the EM and confirm earlier studies, we will first investigate it from reanalysis data. From the seasonally stratified correlation analysis of reanalysis data we conclude that the BF mechanism indeed exists in the TA (figures 1-5 Deppenmeier et al.). Our findings are in line with research performer earlier (Ruiz-Barradas et al. 2000, Keenlyside and Latif 2007, Janssen et al. 2008, Ding et al. 2010). We find the dominant season of the BF to be May, June, and July, and we restrict our analysis from here on to these months. During that time, the patterns are most distinct which facilitates comparison between reanalysis and model output.

An analysis of the seasonal cycle on the variables of interests for the BJ feedback shows that there are biases in the model output (figures 6-7 Deppenmeier et al.), but does this also imply errors in the simulated BF? We have investigated this question by correlating the three variable pairs in the same manner as done for the reanalysis above, and subsequently compare the spatial response patterns to the pattern obtained from reanalysis by performing pattern correlation analysis. Figure 6 shows the pattern correlation between models and reanalysis (vertical axis) versus the correlation value between the two variables of the respective component of the BF (horizontal axis) averaged over two areas of interests. In the following, we use indices as indicators for the western TA (wa4, 4^oN – 4^oS; 40^oW – 20^oW) and the eastern TA (ea4, 4^oN – 4^oS and 20^oW – 10^oE), see also figure 2 in Deppenmeier et al.). In figure 6 the blue shading indicates where the models simulate correctly the BF component.

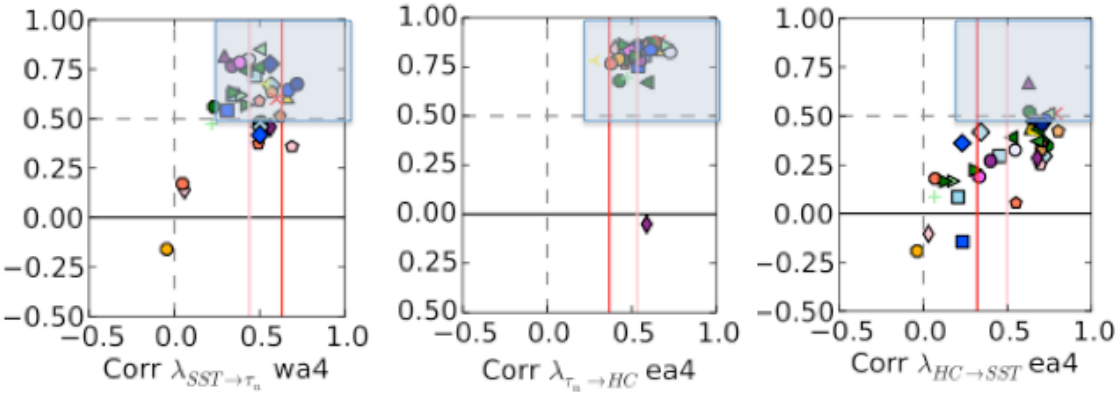

Figure 6: *Pattern correlation between models and reanalysis (MRA) plotted against the correlation value between the two variables of the respective component of the BF averaged over the area of interest. The red line denotes the reanalysis correlation value in the region, the pink line the multi model average. We show the results for June (reanalysis) and July (models). The blue shading indicates where models simulate correctly the BF component.*

From figure 6 it is clear that the $\lambda_{SST \to \tau}$ and $\lambda_{\tau \to HC}$ parts of the BF are reasonably well simulated, notwithstanding the underlying model mean-state biases. However, the third component of the BF $\lambda_{HC \to SST}$ is not correctly simulated. We investigate further this issue by analysing the structure of the variance of the ocean sub-surface temperature within the upper 300m (Figs. 13 and 14 from Deppenmeier et al.). If we compare to ORAS4, the variance structure of the ocean sub-surface temperature is not well represented by models. The latter can explained the deficiencies to represent the HC -> SST relationship. We argue that this may have also implications in the low levels of skill found in the EM in seasonal forecasts systems.

2.2 The WES feedback in CMIP5 models

The WES feedback has also previously investigated in observations, reanalysis and coupled models (Breugem et al. 2006, Mahajan et al. 2009, Munoz et al. 2014), and in some in some theoretical approaches (Vimont 2011). Here we use some models from the CMIP5 database to analyse the representation of the physical mechanism associated to the WES feedback. In our analysis, and given the strong internal variability present in the Tropical Atlantic, only models with three members or more in the historical ensemble have been considered. Other models have been removed from the analysis since all the variables required were not available. Finally, the multi-model dataset is composed by 17 coupled models.

The mechanisms of WES feedback can be explained following Xie and Philander, 1994 as: a north–south SST anomalous gradient will lead to a meridional sea level pressure gradient that can modify the surface winds. Superimposed on the background easterly trade winds, the anomalous westerly winds north of the equator decrease surface wind speed and hence latent heat flux, while the anomalous easterly winds south of the equator increase surface wind speed and associated latent heat fluxes. These changes amplify the initial inter-hemispheric SST difference, and thus provide a positive feedback. According to this, In this work the Wes feedback has been divided in three parts (figure 7): part 1 represents the response to surface winds speed (U) to the SST anomalies (SST->U); part 2 consists of the latent heat (LH) flux modifications by surface winds speed (U->LH); and finally the part 3 is the SST response to latent heat flux forcing (LH->dSST/dt). It is important to note that this study has been performed from monthly mean fields of SST, wind speed and latent heat. The tendency of SSTs (dSST/dt) has been considered for the part 3 of WES feedback.

The study has been performed on a seasonal basis, considering JFM, AMJ, JAS and OND. We have included in our analysis two reanalysis 20CR and NCEP and observed heat fluxes: NOCS (Berry and Kent, 2009), TropFLux (Praveen-Kumar et al. 2012), OAFlux (Yu and Weller, 2008) datasets.

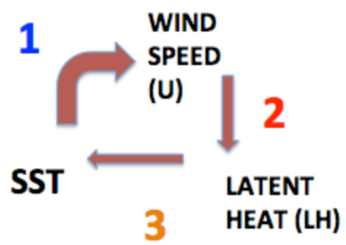

Figure 7: *The WES feedback in three steps: 1) represents the response to surface winds speed (U) to the SST anomalies; 2) consists of the latent heat (LH) flux modifications by surface winds speed (U->LH); and 3) is the SST tendency response to latent heat flux forcing (LH->dSST/dt*

A linear regression based on the least-squares approach has been used to determine each part of the WES feedback described above. To do this, two boxes has been considered in both sides of the equator: the Northern tropical Atlantic box (NTA: 5N-20N, 50W-20W) and the Southern Tropical Atlantic box (STA: 0-20S, 20W-10E). Figure 8 shows the fraction of variance explained by each part of the WES feedback, computed from the linear regression parameters (the fraction of variance explained is given by the squared of the correlation coefficient).

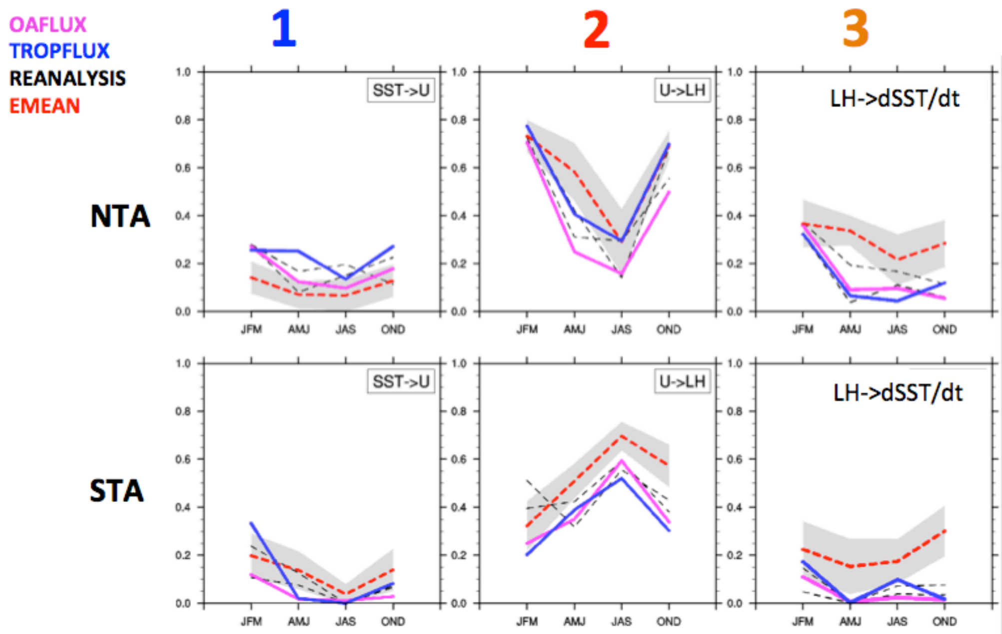

Figure 8: *Fraction (from 0 to 1) of variance explained by the linear regression for each part of the WES feedback according to figure 6 corresponding to the NTA (5N-20N, 50W-20W) (first row) and STA (0-20S, 20W-10E) (second row) boxes respectively. The reanalysis are represented by dash black lines (with no distinction of 20CR and NCEP); OAFlux data by pink lines; TropFlux by orange lines. The multi-model ensemble mean is represented by the thick red line, and the inter-model spread (computed from one standard-deviation) by the gray shading.*

Results show that even for the observations and reanalysis there are strong discrepancies in quantifying the importance of the WES feedback for each part, what makes more difficult the model evaluation. Following figure 8, the results can be summarized as follows:

- Models underestimate the response of the SLP (surface winds) in the NTA throughout the year. To investigate further the hydrostatic equilibrium of the atmospheric boundary layer to underlying SSTs anomalies, higher frequency (daily) data would be necessary. This is beyond the scope of this work.
- The U->LH relationship seems to be more linear in models than in observations in both boxes. This can be due to the use of bulk formulae in coupled models, that uses linear assumptions.
- The most important result: SSTs in models are overreacting to LH flux anomalies in both boxes and for all the seasons of the year.

To further investigate the last point, we have analysed the relationship between the rest of the heat fluxes (net flux, long wave, short wave, sensible heat flux) and the tendency of SSTs. and the net heat flux is mainly dominated by the LH contribution in the tendency of SSTs (not shown).

The evolution of SSTs can be defined the following a simplified equation of the heat budget: $dSST/dt = Qnet/\rho CpH + Advection + Entrainment + Diffusion$

where ρ is the sea water density, Cp is the specific heat capacity of sea water and H is the mixed layer depth. These three can be considered as constants over the regions studied in this work. According to this, our results may suggest that a greater portion of dSST/dt is explained by heat fluxes in models than in observations, and the other purely ocean processes related to ocean dynamic may be underestimated in CMIP5 models.

This is coherent to what has been found by Deppenmeier et al. 2015 on the BF (section 2.1) and to the works by Nnamchi et al. 2015 and Ding. et al. 2015 that suggest that the role of ocean dynamics driving SST variability in the Tropical Atlantic is not well represented by state-of-the-art coupled models. This will be more detailed in section 2.3.

2.3 The role of the ocean dynamics driving SST variability

(Ding et al. 2015b, Nnamchi et al. under revision, Planton et al. under revision)

a) Partial coupled model experiments (Ding et al. 2015b)

We have examined the impact of SST bias on the representation of the interannual variability during boreal summer over the equatorial Atlantic. For this, we have developed and run two suites of partially coupled model (PCM) experiments with (PCM-Hflux) and without (PCM-STD) surface heat flux correction by using the Kiel Climate Model (KCM). In the experiments, surface wind stress anomalies are specified from observations while the thermodynamic coupling between the atmospheric and oceanic components is still active as in the fully coupled model. More details on the experiment can be found in Ding et al. 2015b.

We investigate the impact of subsurface temperature anomalies on local SST variations by calculating the regression of SST anomalies onto local SSH (Sea Surface Height) anomalies during boreal summer (figure 9). Here, SSH is used as a proxy for subsurface temperature variations. The regression between the SSH and SST has been computed from observations (figure 9a), the PCM experiment with no heat flux correction, PCM-STD (figure 9b), and the partially coupled model simulation with flux correction (PCM-Hflux, figure 9c). Regression values calculated from observations show a link between subsurface and SST variations (figure 9a), consistent with previous studies (Keenlyside and Latif 2007, Deppenmeier et al. 2015). In contrast to the observations, subsurface and SST variations in PCM-STD are coupled in the western tropical Atlantic but not in the east (figure 9b). This seems to be associated with the climatological mean surface winds being biased westerly in the east (not shown), implying Ekman downwelling along the equator, meaning that subsurface temperature anomalies cannot easily impact SST variability in the east (Ding et al., 2015). However, the PCM-Hflux configuration (figure 9c) captures well the observed relation between subsurface temperature and SST variability in the eastern equatorial Atlantic in both amplitude and explained variance, and the spatial pattern is roughly consistent with the one seen in observations (figure 9a). The success for capturing the link is probably because of the reduced westerly wind bias and the improved upper ocean temperature structure in PCM-Hflux compared to PCM-STD (Figures 1a and S1 in Ding et al. 2015b). It is obvious that PCM-Hflux (figure 9c) still exhibits an unrealistic link between SST and SSH in the western equatorial Atlantic similar to but weaker than in PCM-STD (figure 9b). This is probably because it is not possible to cure model bias in all aspects through only reducing the warm bias at the sea surface using surface heat flux correction. So far, we have focused on the role of subsurface temperature variations, an important element of the

Bjerknes feedback (Keenlyside and Latif , 2007). Nevertheless, some other ocean processes may also contribute to SST variability, and their role in global climate models is also uncertain. This is coherent to the findings described in sections 2.1 and 2.2 on feedbacks mechanisms.

In conclusion: To derive a complete picture of the contribution of ocean dynamics in stare-of-the-art coupled models a full heat budget analysis is required for both coupled models and stand-alone ocean models in order to assess the impact of the air-sea coupling. Heat budget in stand-alone ocean model has been already performed by Planton et al. (see part c). But a multi-model approach should be undertaken in future studies.

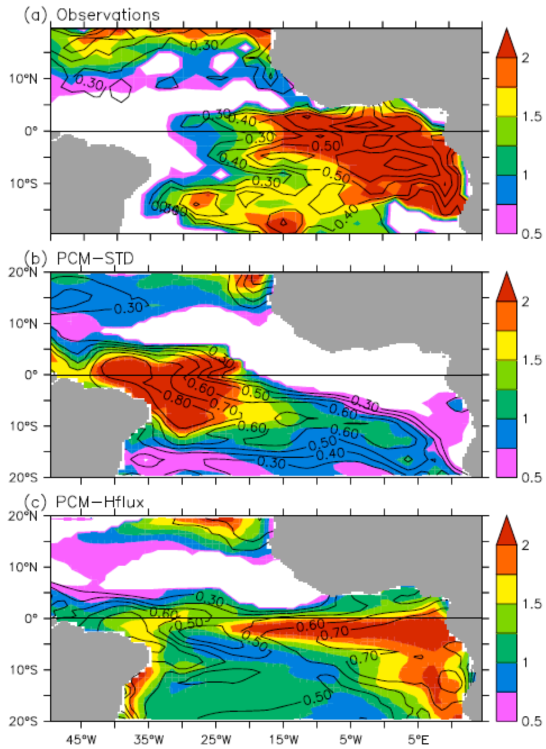

__Figure 9:__ The regression (shading) of seasonal mean (JJA) SST anomalies onto local seasonal mean (JJA) sea surface height (SSH) anomalies calculated from (a) observations, (b) PCM-STD, and (c) PCM-Hflux. The contours are the explained variances, and their interval is 0.1. In Figure 6a, observed reconstructed SST [Rayner et al., 2003] is employed and SSH from satellite (http://www.aviso.oceanobs.com/) is used. The unit of the regression coefficients is C/(10 cm). From Ding et al. 2015b.

b) Fully coupled versus slab-ocean models (Nnamchi et al. in revision)

In this work we investigate the role of the dynamical coupling between the ocean and atmosphere in generating the SSTs equatorial Atlantic variability. We explore this question by comparing simulations of two sets of experiments using 12 different climate models from the CMIP3 database (Meehl et al. 2007). The first set of experiments is based on state-of-the-art, fully coupled general circulation models (Full-CGCMs, hereafter), and in the second set, dynamical feedbacks are disabled by thermodynamically coupling the atmosphere to a 50m deep slab of motionless ocean (Slab-CGCMs hereinafter).

To represent SST interannual variability in the equatorial Atlantic, we compute the standard deviation (σ{SST}') of the Atlantic Niño Index (3^oS-3^oN, 0-20^oW) from Slab-CGCMs and Full-CGCMs considering June-July-August months (JJA). Figure 10a shows the scatter plot for σ{SST}' in Full-CGCMs versus Slab-CGCMs. For comparison to the Pacific, we include the σ{SST}' for the Pacific Niño3 index (5^oS-5^oN, 90-150^oW) computed from DJF (boreal winter) (Figure 10b). From figure 10a, the σ{SST}' of the Atlantic Niño of the Full-CGCMs (representing the total variability of the equatorial Atlantic ocean-atmosphere coupled system) is linearly dependent on the σ{SST}' of the Slab-CGCMs with no interactive ocean dynamics. The multi-model correlation coefficient is 0.96, corresponding to 92% of the explained variance. In comparison, the equatorial Pacific variability exhibits more scatter with an explained variance of only 3%. This implies that while dynamical coupling in the equatorial Atlantic acts to amplify the σ{SST}', coupled dynamics in the Pacific tends to modify the SST variability.

We determined the proportions of the observed SST variability over the eastern equatorial Atlantic Ocean by computing the JJA ratios of the modelled σ{SST}' to recent historical observations (NOAA, Smith et al. 2008) for the period 1984-2013. Figure 10c shows the model/observations ratio in σ{SST}' for the Atlantic Niño index. For the Slab-CGCMs ensemble, 10 models have ratios of >0.50, with the 12 Slab-CGCMs ensemble-mean of 68 ± 23%, suggesting that thermodynamic processes dominate the equatorial Atlantic interannual SST variability (figure 10c). Similar ratios were calculated for the boreal winter peak season of the equatorial Pacific using the Niño3 index. The corresponding ensemble-mean contribution of thermodynamic feedbacks for the Niño3 region is considerably lower at ~32 ±11% (figure 10d).

The Full-CGCM ratios are also plotted on the same axes of figure 10 c-d. Some models with deep mixed layer of generally >50 m (e.g., CCSM3, CGCM3.1_T47 and CGCM3.1_T63) tend to underestimate the observed σ{SST}'. In contrast, for those models in which the thermodynamic component generate σ{SST}' close to observations (e.g., GFDL-CM2.0, GFDL-CM2.1, INM-CM3.0 and UKMO-HadGEM1), coupling to ocean dynamics leads to an overestimation of the Atlantic Niño σ{SST}', given that the mixed layer depths are not much different from the observed. The ensemble-mean of the Full-CGCMs reproduces the temporal variability of the equatorial Atlantic SST as may be expected from the consistency of the modelled mean mixed layer depths with observations.

We show here that thermodynamic mechanisms play dominant roles in both sets of experiments, accounting for 68 ± 23% of observed equatorial Atlantic interannual SST variability in the Slab-CGCMs, through the WES feedback. The impact of coupling to a dynamical ocean model is to amplify the variability and the Niño-like spatial structure. We conclude that, governed by stochastic atmospheric forced heat and moisture fluxes, the Atlantic Niño is not different from a first-order autoregressive (AR(1)) process.

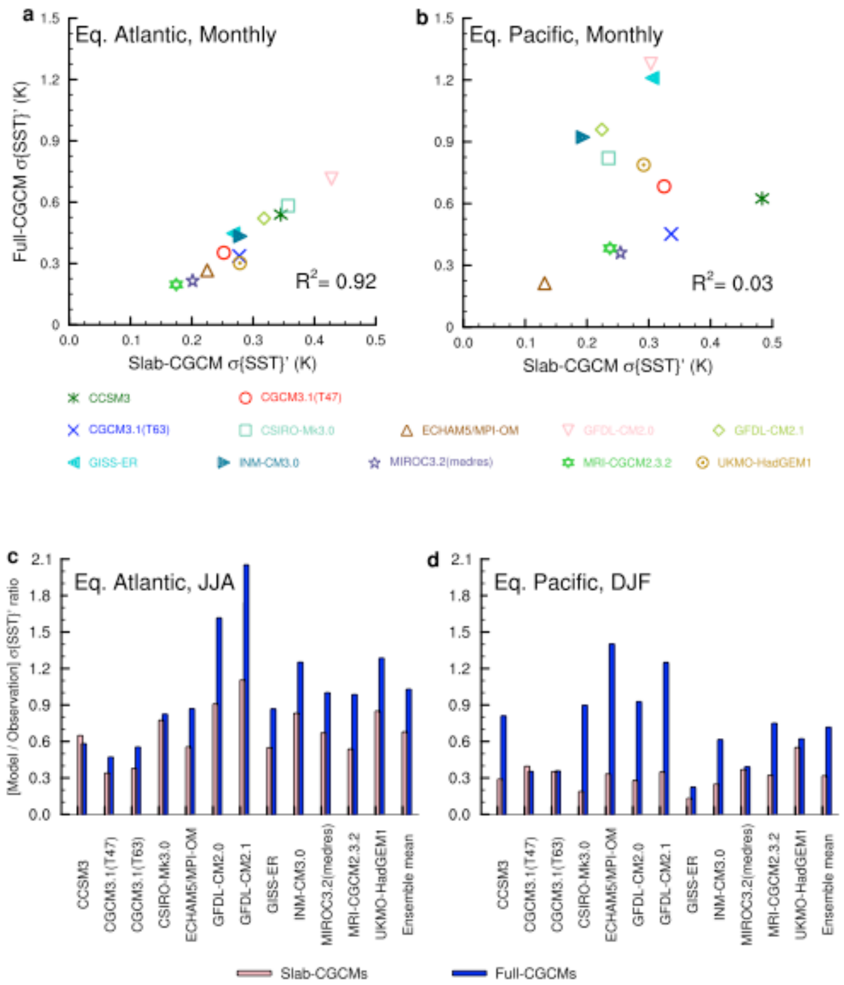

Figure 10: *Multi-model linearity of thermodynamic feedbacks in the equatorial Atlantic and Pacific oceans and modelled proportions of the observed variability. a-b, Relationship between the monthly Atlantic Niño (3S-3N, 0-20W) and Pacific Niño3 (5S-5N, 90-150W) σ{SST}' from Slab-CGCMs and Full-CGCMs. c-d, Atlantic Niño and Pacific Ni.o-3 model/observation ratio of the σ{SST}'. Blue bars denote the ratio for Full-CGCMs; light-pink, Slab-CGCMs. A ratio of >1.0 denotes an over-estimation of observed variability of ~0.40 K and 0.95 K for the Atlantic Niño and Pacific Niño3, respectively. Panels c and d are based on the JJA and December-January-February (DJF) seasonal means, respectively. From Nnamchi et al. 2015.*

c) Assessment of the representation of seasonal and interannual variability of a ocean component in a coupled model (Planton et al. in revision)

We have investigated the performance of the CNRM-CM ocean model (NEMO, Madec et al. 1998) in representing the equatorial Atlantic interannual variability. Our goal is to evaluate the ocean model realism being forced by observed atmospheric forcing. This study has been done in collaboration with WP5.

This work aims at evaluating the NEMO ocean model realism being forced by observed atmospheric forcing. Two atmospheric forcing have been used to drive the NEMO-ORCA1 configuration (with 42 vertical levels): the CORE-II forcing and an ERA-Interim forcing (slightly corrected for radiation biases).

We show that the variability of the surface temperature and the ocean heat content in the upper 300 meters is reasonably well simulated whatever forcing is used. The location of strong equatorial interannual variability shown at the PIRATA buoy at 35°W-0N between 80m and 120m depth is reproduced in the NEMO simulation, albeit with a weaker amplitude (figure 11). Accordingly, the model reproduces well the South Equatorial Current (SEC) and the Equatorial Under Current (EUC) extents. The vertical core of the EUC is near 60 m depth at 23°W-0N as observed at the PIRATA buoy. The strength of the EUC is however largely underestimated by more than 40% compared to the PIRATA measures but it is of the same order as in ocean reanalysis products. Generally, there is no clear improvement of using one forcing product or the other.

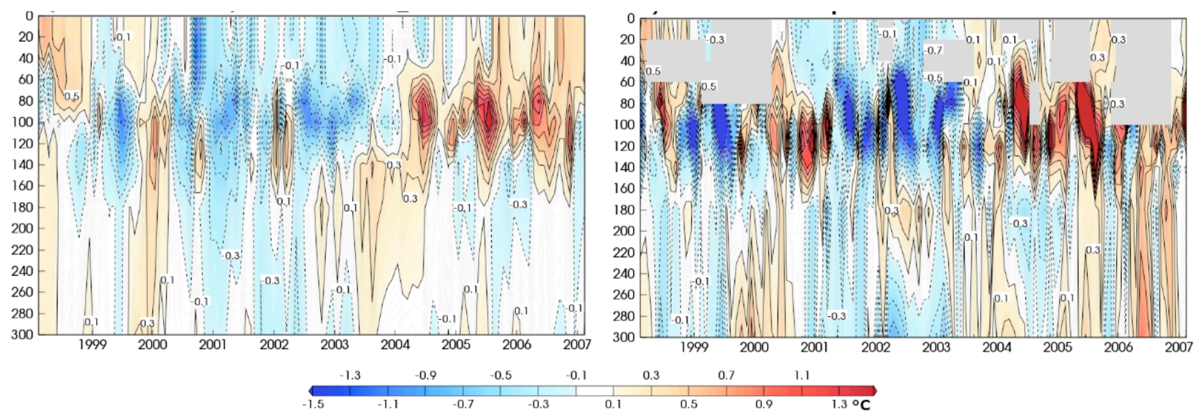

Figure 11: *Hovmoeller diagram time versus depth of the anomaly of ocean temperature to the mean seasonal cycle at the PIRATA buoy located at 35°W0°N (right) and for the NEMO-ORCA1 (left).*

A comprehensive heat budget of the mixed layer has been performed in the NEMO simulations (Figure 12) and this has shown that the heating of the mixed layer by the surface flux (25-55W.m^{-2}) is weaker in the model than estimates derived from observations that range from 40W.m^{-2} to 95W.m^{-2} (Foltz et al., 2003, Hummels et al., 2014, Schlundt et al., 2014). It has been shown that it is due to an excessive penetration of the solar radiation in the ocean, the mixed layer being relatively shallow in the region, the solar radiation impacts also the ocean under the mixed layer. This effect is overestimated in the model. To increase the solar radiation heating in the mixed layer, we have adapted the absorption coefficients used in the model by using the coefficients estimations given in Wade et al. (2011). Secondly, we have used a chlorophyll map so that the light penetration depends on the geographical location and better match the observed spatial variability. Given these adaptations, the air-sea flux impact on the mixed layer budget has increased to the range 38-

95W.m^{-2} in agreement with observed estimates, and the seasonal cycle of this term is better reproduced.

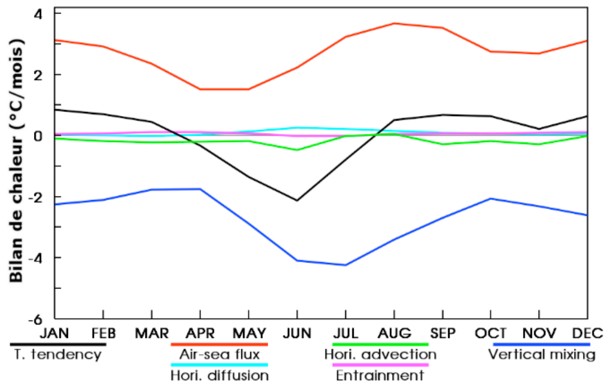

Figure 12: *Mean seasonal cycle of the mixed layer heat budget in the box [15°W-6°W ; 4°S-1°N] averaged over 1982-2007 in the NEMO-ORCA1 model, after adaptation of the solar penetration effects.*

Part of this work has been submitted for publication in Climate Dynamics (Planton et al., 2015).

3.Relationship between the mean state and the representation of the variability.

N. Keenlyside[1], M. Latif[2], C. Prodhomme[3]
[1] UiB, Bergen, Norway
[2]GEOMAR, Kiel, Germany
[3]IC3, Barcelona, Spain

In this section we investigate how the errors in the mean state affect the representation of Tropical Atlantic Variability. We have focused rather in the equatorial Atlantic variability, represented by the Equatorial Mode (EM), Zonal mode (ZM) or Atlantic Niño. The first part of this study uses the existing simulations from CMIP5 and applies statistical analysis to obtain empirical relationships between the mean state biases and the representation of the equatorial Atlantic variability (3.1). The second part uses a numerical approach in which the mean state of a coupled model is modified, in order to assess its impact of the equatorial Atlantic variability (3.2). The latter work has been published in a recent work by Ding. et al 2015a.

3.1 Relation between SST seasonal cycle and variability in the equatorial Atlantic

Huge efforts are done to improve the representation of coupled model mean state, especially in the tropical Atlantic. The reduction of the mean bias is expected to lead to improvements in other aspects of the simulation such as the representation of interannual and intraseasonal variability. However, the relation between the correct representation of the mean state and the interannual variability has been seldom studied (Richter et al. 2014), where the biases are huge in most of the coupled model (Toniazzo and Woolnough 2014). The present study is aimed to investigate if there is a relation between the representation of the mean bias in the equatorial Atlantic and the representation of the equatorial Atlantic variability (Atlantic Niño). For this purpose, we are using the CMIP5 coupled model database the model used are summarized in Table 3.

Model	Number of member
bcc	1
hadcm3	10
miroc4	3
miroc5	3
mri-cgcm	1
cnrm-cm	1
can-cm4	10
MPI-OM	3
GFDL	10
EC-Earth 2.3	10
IPSL	4
CMCC-CM	1

Table 3: *Summary of the information for the different models used in this work. For all the models model the time period used is 1961-2006.*

In order to assess if there is a first order relationship between the mean state and the biases in the TA, figure 13 shows the different aspects of the simulation of the Atl3 box in the CMIP5 models (20W-0W, 3S-3N, Rodriguez-Fonseca et al. 2009): seasonal cycle, monthly standard deviation and bias. This figure shows that most of the models exhibit a large warm bias in summer (figure 13c) and this is mainly linked with a delayed and too weak development of the cold tongue in this region (figure 13a and c). Only few models manage to reproduce the peak of standard deviations during summer in the equatorial Atlantic and the only model having a correct amplitude of the standard deviation in summer is the bcc coupled model (Figure 13b and d). It is interesting to note, that this model have a relatively large bias in the same box (figure 13c), suggesting that there is no clear relation between the JJA climatological SST in the Atl3 box and the standard deviation. In order to confirm this hypothesis, figure 13e shows the scatter plot between the JJA SST climatology and the standard deviation averaged in the Atl3 box. This figure 13e clearly confirms that there is no direct relation between the representation of the JJA mean SST and the amplitude of interannual variability in the Atl3 region. However, if instead of looking at the amplitude of the bias in the Atl3 region, we look at the strength of the cold tongue development in the model, in other word the different between July and April SST average in Atl3, a clear relation appears with the amplitude of the standard deviation (figure 13f). The p-value of this regression is 0.002, which shows that this relation is significant. This result suggests that the important parameter for a coupled model to simulate a realistic equatorial Atlantic variability is to be able to represent a realistic cold tongue development between spring and summer in this region.

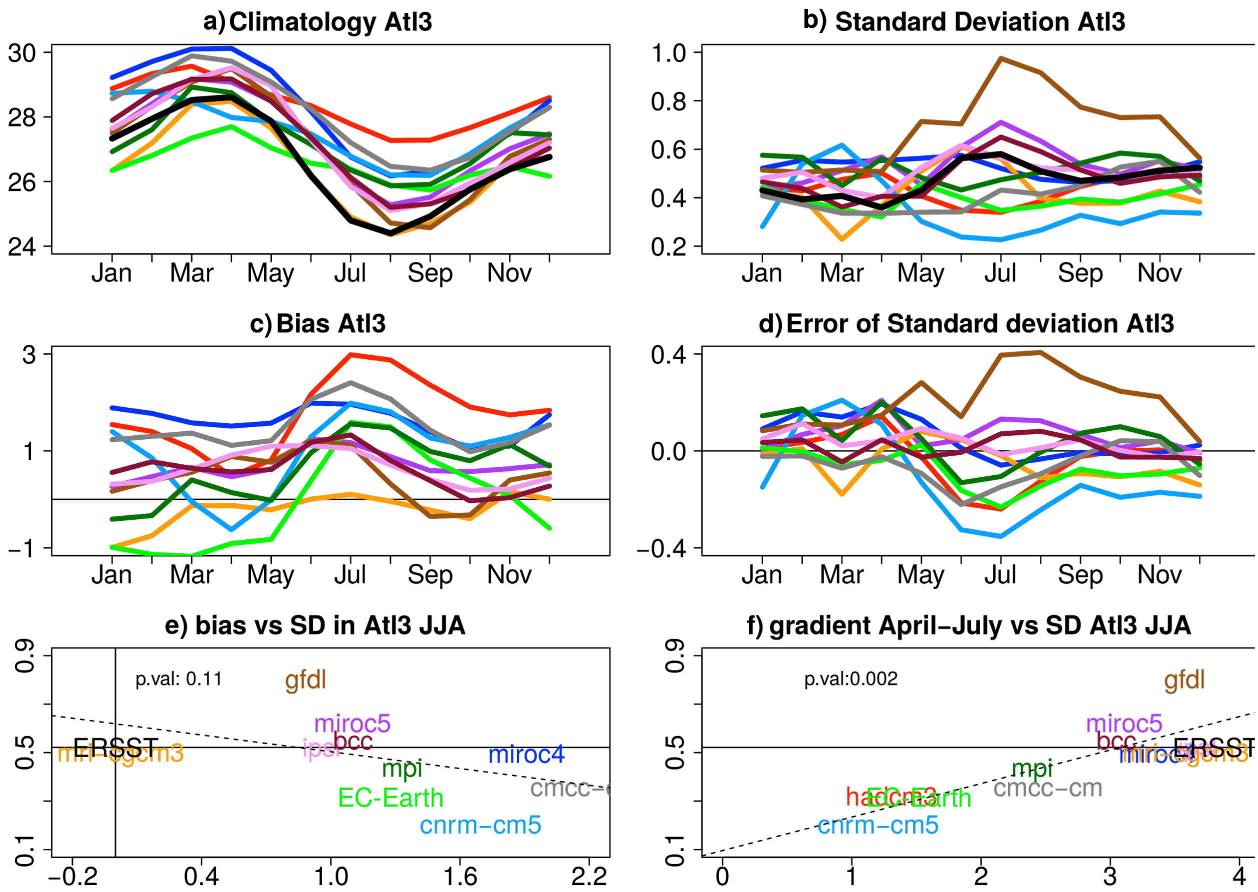

Figure 13: *a) Climatological seasonal cycle of the SST averaged in the Atl3 box (20ºW0ºW-3ºS3ºN). b) Standard deviation in the Atl3 averaged over the different members. c) Difference between CMIP5 coupled model climatological SST minus climatological observed SST in the Atl3 box. d) Difference Standard deviation in the Atl3 averaged over the different members minus the observed standard deviation. e) Scatter plot of the relation between mean bias in JJA in Atl3 (x-axis) and the standard deviation in Atl3 (y-axis). f) Scatter plot of the relation between the SST in April minus the SST in July in Atl3 (x-axis) and the standard deviation in Atl3 (y-axis).*

3.2 The impact of mean state errors on equatorial Atlantic interannual variability in a climate model

(Ding et al. 2015a)

Theoretical and observational studies indicate that the mean state has a strong prein on interannual variability in the Tropical Pacific (Battisti and Hirst, 1989; Fedorov and Philander, 2001; Lubbecke and McPhaden, 2013). However, it is still not clear what is the influence of the warm SST bias on the interannual variability in the Equatorial Atlantic given that some coupled model can capture the Equatorial Mode (EM) or Atlantic Niño, while others cannot, as reported in recent studies (Munoz et al., 2012; Liu et al., 2013; Richter et al., 2014). Here we investigate new climate model configurations to address the following scientific questions:

- Can simulation of interannual variability be improved in a coupled model if the mean bias is reduced?
- What are the influences of the SST warm bias on the mechanism of Atlantic Niño?

We address the questions presented above by investigating a set of experiments performed with different configurations of the KCM (Kiel Climate Model) with perturbed parameters and momentum flux correction. Three experiments are performed and analysed: (1) a reference run using the models standard (like-CMIP5) configuration (REF) with Tropical Atlantic bias similar to most state-of-the-art climate models; (2) a run that employs modifications in the physical parameterization of the atmospheric model that mainly influence the turbulent transfer of heat and moisture at the ocean surface, leading to an improved simulation of the Atlantic mean state (MOD); and (3) a momentum flux corrected version of the KCM using its standard configuration (Mflux) that exhibits climatological SST and thermocline depth variations similar to observations. The three model configurations are used in this study because they represent Equatorial Atlantic climate to different degrees of fidelity. More description on the experimental set-up can be found in Ding et al. 2015a.

Mflux is used to assess the impact of (somewhat artificially achieved) near perfect simulation of the climatology on interannual variability while MOD provides an indication of the impact of more modest reductions in mean state error. The three model configurations are compared against observations. In this work we use the HadISST1.1 (Rayner et al. 2003) data set for observed SSTs and WOA05 (Locarnini et al. 2006) for subsurface ocean temperature.

We investigate the BF (Bjerkness feedback) in the three KCM configurations (see figs. 6-8 in Ding et al. 2015a). We show that the three elements of the Bjerknes feedback exist to some degree in all the three experiments. In the REF, the first ($\lambda_{SST\rightarrow\tau}$) and third ($\lambda_{\tau\rightarrow HC}$) elements are much weaker than those in MOD and Mflux, consistent with less variance of the EM in REF. In Mflux, the first element of the BF is slightly stronger than observed, and much stronger than in MOD. In MOD and Mflux, the second and third elements ($\lambda_{HC\rightarrow SST}$) of the BF resemble each other. The stronger BF in Mflux than in MOD is consistent with the ZM greater explained in Mflux (figure 5 in Ding et al. 2015a).

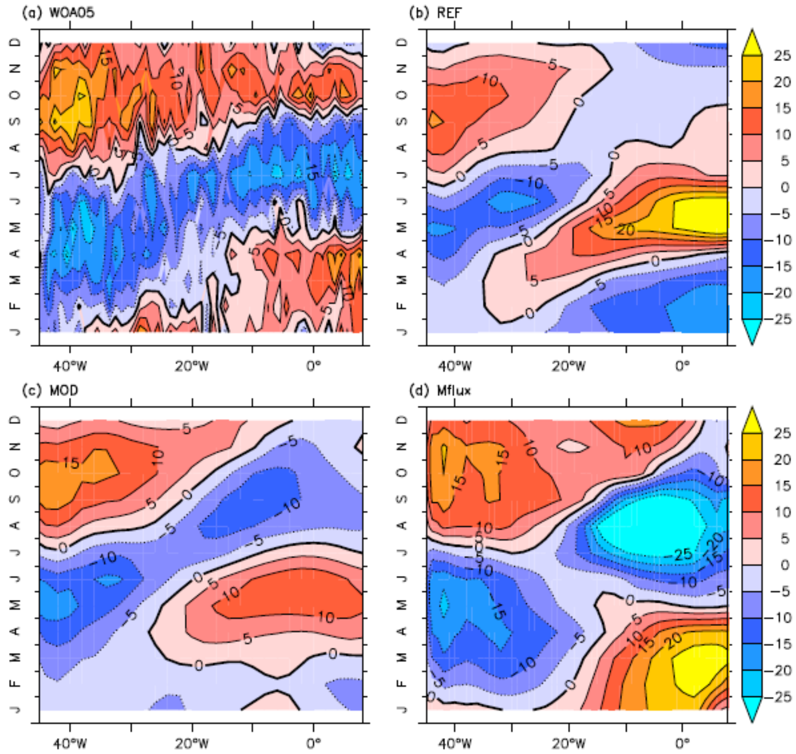

Figure 14: *Longitude-time sections of biases of surface zonal winds (contours shown in left), SST (shading shown in left side) and Z20 (right side) at the equator (averaged between 2S and 2N) calculated from (a and b) REF, (c and d) MOD, and (e and f) Mflux experiments. The units of surface zonal winds, SST, and Z20 are meters.*

Looking now at the seasonality of the equatorial SST variability, Figure 14 shows the longitude-time sections of seasonal cycle of isotherme-20deg depth (Z20 hereinafter) at the equator (averaged between 2^{o}S and 2^{o}N) calculated from the three experiments and from WOA05. In REF, the mean bias is so large in May and June that the seasonal cycle of Z20 in the east is almost opposite to that in the observations (figure 14 a and b). The unrealistically deep thermocline in the east inhibits upwelling of cold water, causing the maximum warm SST bias during boreal summer (JJA). The seasonal evolution of the bias in REF is consistent with that in Richter and Xie (2008), as described in Wahl et al. (2009) for the KCM. While the biases in MOD are somewhat reduced compared with REF, they exhibit similar seasonal evolution: The seasonal cycle of Z20 is still almost opposite to that in observations (figure 14 a and c). Mflux displays the best phase of the seasonal cycle of Z20 of all the simulations, with shallower thermocline from June to September in the east (figure 14 a and d). Nevertheless, the simulated seasonal cycle of Z20 is stronger than observed and some moderate SST errors remain.

Monthly standard deviations of SST at the equator shows there are also marked differences in the seasonality of SST variability among the simulations and observations (figure 15). In observations, the maximum SST variability is in the east from June to July (figure 15a), as has been reported by many previous studies (Xie and Carton, 2004; Keenlyside and Latif, 2007; Richter et al., 2014). In REF, SST variability peaks around May, but the maximum is found in the central Atlantic to the west of the observed maximum (figure 15a and 15b). In MOD and Mflux, SST variability is located mainly in the eastern part of the Equatorial Atlantic and is more consistent with observations than REF. However, MOD simulates maximum SST variability from July to September, about 2 months later than that in the observations and Mflux. This may be associated with the delayed seasonal cycle of Z20 (figure 14c). Mflux has the best simulation in terms of phase, capturing the maximum SST variability in June and July.

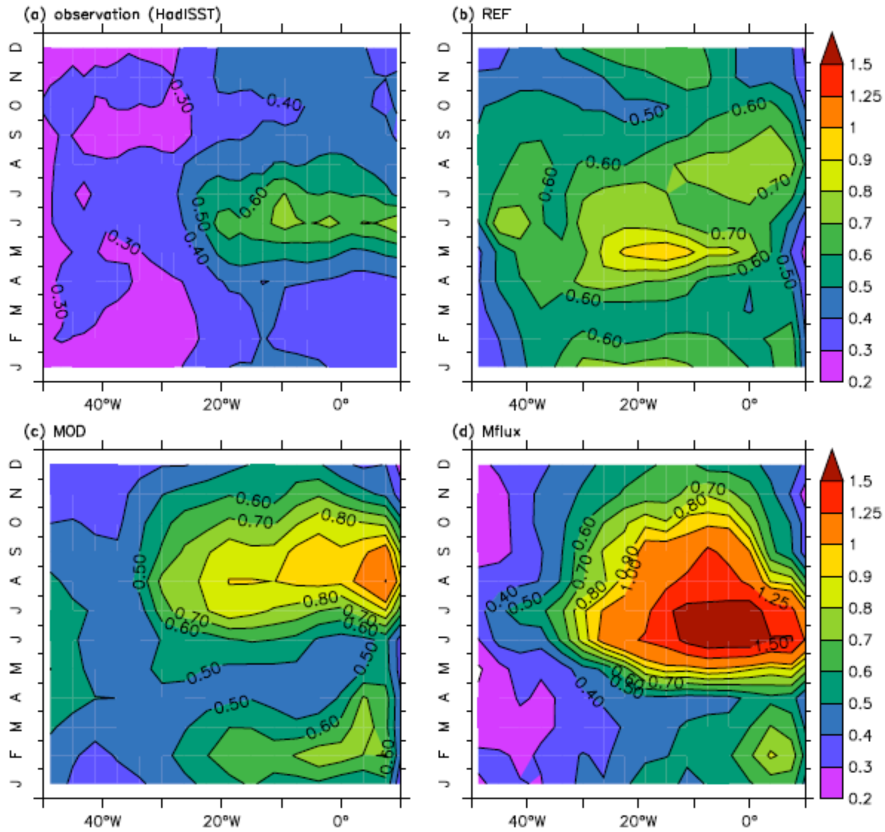

Figure 15: *Longitude-time sections of monthly stratified standard deviation of SST along the equator (averaged between 2S and 2N) calculated from (a) observation (Rayner et al., 2003), (b) REF run, (c) MOD run, and (d) Mflux run. The unit is Celsius.*

Our results show that Mflux in the best performing KCM configuration to represent BF and SST interannual variability. In summary, from this study suggest that a better simulation of interannual variability in the Equatorial Atlantic can be achieved through improving the mean state in coupled ocean-atmosphere general circulation models. This, however, is not trivial, because the climate system in the equatorial sector is strongly coupled, giving rise to a high sensitivity to errors in individual model components so that biases in different component models and regions could be linked with each other [Wang et al., 2014]. With respect to seasonal forecasting, momentum flux correction could be an option, as long as the coupled models suffer from large biases. Nevertheless, as shown here momentum flux correction cannot fully correct ocean-atmosphere feedbacks.

References

PREFACE (D7.1) references are in bold blue

Balmaseda, M. A., Mogensen, K. and Weaver, A. T., 2013: Evaluation of the ECMWF ocean reanalysis system ORAS4. Q.J.R. Meteorol. Soc., 139: 1132–1161. doi: 10.1002/qj.2063

Battisti, D. S., and A. C. Hirst, 1989 : Interannual variability in a tropical atmosphere-ocean model: Influence of the basic state, ocean geometry and nonlinearity, J. Atmos. Sci., 46(12), 1687–1712, doi:10.1175/1520-0469

Berry, D. I. and E. C. Kent, 2009: A New Air-Sea Interaction Gridded Dataset from ICOADS with Uncertainty Estimates. Bulletin of the American Meteorological Society, 90(5), 645-656 (DOI: 10.1175/2008BAMS2639.1).

Breugem, W-.P.*,* W. Hazeleger*, and* R. J. Haarsma*,* 2006*:* Mechanisms of northern tropical Atlantic variability and response to CO_2 doubling*,* J. Clim.*, 20,* pp. 2691-2705.

Carton J A, Cao X, Giese B S and Da Silva A M, 1996 : Decadal and interannual SST variability in the tropical Atlantic Ocean, J. Phys. Oceanogr, 26, 1165–1175

Chang, P., Ji, L., Li, H., 1997: A decadal climate variation in the tropical atlantic ocean from thermodynamic air-sea interactions, Nature, 385(6616), 516–518

Chang P, Fang Y, Saravanan R, Ji L and Seidel H 2006 The cause of the fragile relationship between the Pacific El Niño and the Atlantic El Niño, Nature, 443, 324-328

Chiang J. C. and D.J. Vimont, 2004: Analogous Pacific and Atlantic Meridional Modes of Tropical Atmosphere–Ocean Variability, J. Climate, 17, 4143-4158.

Compo, G.P., J.S. Whitaker, P.D. Sardeshmukh, N. Matsui, R.J. Allan, X. Yin,B.E. Gleason, R.S. Vose, G. Rutledge, P. Bessemoulin, S. Bronnimann, M. Brunet, R.I. Crouthamel, A.N. Grant, P.Y. Groisman, P.D. Jones, M.C. Kruk, A.C. Kruger, G.J. Marshall, M. Maugeri, H.Y. Mok, O. Nordli, T.F. Ross, R.M. Trigo, X.L. Wang, S.D. Woodruff, S.J. Worley, 2011: The Twentieth Century Reanalysis Project. Quarterly J. Roy. Met. Soc., 137, 1-28 (DOI: 10.1002/qj.776).

Dee et al., 2011: The ERA-Interim reanalysis: configuration and performance of the data assimilation system, Q.J.R. Meteorol. Soc., Vol. 137: 553-597, DOI: 10.1002/qj.828

Deppenmeier A-L, Haarsma R J and Hazeleger W, 2015: The Bjerknes feedback in the tropical Atlantic, *Climate Dynamics,* submitted.

DeWitt, D.G., 2005: Diagnosis of the tropical atlantic near-equatorial sst bias in a directly coupled atmosphere-ocean general circulation model. Geophys. Res. Lett. 32(1)

Ding H, N. Keenlyside, and M. Latif (2010): Equatorial Atlantic interannual variability : The role of heat content, J. Geophys. Res., 115, C09020, doi:10.1029/2010JC006304

Ding H, Keenlyside N, Latif M, Park W, Wahl S., 2015a: The impact of mean state errors on equatorial Atlantic interannual variability in a climate model. J Geophys Res Oceans, 120, 1133-1151.

Ding, H., Greatbatch R., Latif M. and W. Park, 2015b: The impact of sea surface temperature bias on equatorial Atlantic interannual variability in partially coupled model experiments, submitted to GRL.

Fedorov, A. V., and S. G. Philander, 2001: A stability analysis of tropical ocean-atmosphere interactions: Bridging measurements and theory for El Niño, J. Clim., 14(14), 3086–3101, doi:10.1175/1520-0442

Foltz GR, Grodsky SA, Carton JA, McPhaden MJ, 2003: Seasonal mixed layer heat budget of the tropical Atlantic Ocean. J. Geophys. Res., 108(C5):3146. doi: 10.1029/2002jc001584.

Gonzalez-Reviriego, N., C. Rodriguez-Puebla, and B. Rodriguez-Fonseca, 2014: Evaluation of observed and simulated teleconnections over the Euro-Atlantic region on the basis of partial least squares regression, Climate Dynamics, 44.11-12 : 2989-3014.

Hummels R, Dengler M, Brandt P, Schlundt M, 2014: Diapycnal heat flux and mixed layer heat budget within in the Atlantic Cold Tongue. Clim. Dyn., 43(11):3179-3199, doi: 10.1007/s00382-014-2339-6

Janssen, M.F., Dommenget, D., Keenlyside, N., 2008 : Tropical atmosphere-ocean interaction in a conceptual framework. J. Climate, 22, 550-567

Kalnay et al., 1996: The NCEP/NCAR 40-year reanalysis project, Bull. Amer. Meteor. Soc., 77, 437-470

Keenlyside, N.S., Latif, M., 2007 : Understanding equatorial atlantic interannual variability. J. Climate 20, 131–142 URL http://dx.doi.org/10.1175/JCLI3992.1

Madec G, Delecluse P, Imbard M, Levy C, 1998 : Opa 8.1 ocean general circulation model reference manual. Note du Pole de modelisation. Institut Pierre-Simon Laplace:11

Mahajan, S., Saravanan, R., Chang, P., 2009: The role of the wind-evaporation-sea surface tem- perature (wes) feedback in air–sea coupled tropical variability. Atmos. Res. 94(1), 19–36

Martin-Rey M, I. Polo. B. Rodriguez-Fonseca, T. Losada and A. Lazar, 2015: On the different configurations of the Atlantic Nino phenomenon under negative AMO phases, to be submitted

Meehl, G. A. et al., 2007 : The WCRP CMIP3 Multimodel Dataset: A New Era in Climate Change Research. Bull. Amer. Meteorol. Soc., 88, 1383–1394

Munoz, E., Weijer, W., Grodsky, S.A., Bates, S.C., Wainer, I., 2012: Mean and variability of the tropical atlantic ocean in the ccsm4. J. Climate 25(14), 4860–4882

Nnamchi, H. C., J. Li, and R. N. C. Anyadike, 2011: Does a dipole mode really exist in the South Atlantic Ocean?, J. Geophys. Res., 116, D15104, doi:10.1029/2010JD015579.

Nnamchi, H. C., J. Li, F. Kucharski, I-S. Kang, N. S. Keenlyside, P. Chang, and R. Farneti, 2015: Thermodynamic controls of the Atlantic Niño. *Nature Communications,* Submitted.

Liu, H., C. Wang, S.-K. Lee, and D. Enfield, 2013 : Atlantic warm pool variability in the CMIP5 simulations., J. Clim., 26(15), 5315–5336, doi: 10.1175/JCLI-D-12-00556.1.

Locarnini, R., A. Mishonov, J. Antonov, T. Boyer, and H. Garcia, 2006 : World Ocean Atlas 2005, volume 1: Temperature, in NOAA Atlas NESDIS 61, edited by S. Levitus, 182 pp., U.S. Gov. Print. Off., Washington, D. C.

Lubbecke, J. F., and M. J. McPhaden, 2013 : A comparative stability analysis of Atlantic and Pacific Ni~no modes, J. Clim.

Planton, Y., A. Voldoire, H. Giordani, G. Caniaux, 2015: Main processes of interannual variability of the Atlantic cold tongue, Clim. Dyn., under revision.

Praveen Kumar, B., J. Vialard, M. Lengaigne, V. S. N. Murty, M. J. McPhaden, 2012: TropFlux: Air-Sea Fluxes for the Global Tropical Oceans - Description and evaluation, Climate Dynamics, 38, 1521-1543, doi:10.1007/s00382-011-1115-0

Rayner, N., D. Parker, E. Horton, C. Folland, L. Alexander, D. Rowell, E. Kent, and A. Kaplan (2003), Global analyses of sea surface temperature, sea ice, and night marine air temperature since the late nineteenth century, J. Geophys. Res., 108(D14), 4407, doi:10.1029/2002JD002670.

Richter, I., and S. Xie, 2008 : On the origin of equatorial Atlantic biases in coupled general circulation models, Clim. Dyn., 31(5), 587–598, doi:10.1007/s00382-008-0364-z.

Richter I., Xie S.P., Behera S.K., Doi T. and Y. Masumoto, 2014: Equatorial Atlantic variability and its relation to mean state biases in CMIP5, Clim. Dyn., DOI: 10.1007/s00382-012-1624-s.

Rodríguez-Fonseca, B., I. Polo, J. García-Serrano, T. Losada, E. Mohino, C. R. Mechoso, and F. Kucharski, 2009: Are Atlantic Niños enhancing Pacific ENSO events in recent decades?, Geophysical Research Letters, 36 , L20,705.

Ruiz-Barradas, A., Carton, J.A., Nigam, S., 2000 : Structure of interannual-to-decadal climate variability in the tropical atlantic sector. Am. Met. Soc. 13

Smith, T. M. et al. 2008 : Improvements to NOAA's historical merged land–ocean surface temperature analysis (1880–2006). J. Clim. 21, 2283–2296

Schlundt M, Brandt P, Dengler M, Hummels R, Fischer T, Bumke K, Krahmann G, Karstensen J , 2014: Mixed layer heat and salinity budgets during the onset of the 2011 Atlantic cold tongue. J. Geophys. Res.: Oceans, 119:7882-7910. doi: 10.1002/2014JC010021

Servain J., Wainer I., McCreary J.P. and A. Dessier, 1999 : Relationship between the equatorial and meridional modes of climate variability in the Tropical Atlantic, Geophys. Res. Lett., 26, 458 – 488.

Taylor, K. E., J. R. J. Stouffer, and Gerald A. Meehl, 2012: An Overview of CMIP5 and the Experiment Design, Bull. Amer. Meteor. Soc., 93, 485–498. doi: http://dx.doi.org/10.1175/BAMS-D-11-00094.1

Toniazzo, T., and Woolnough, S., 2014: Development of warm SST errors in the southern tropical Atlantic in CMIP5 decadal hindcasts. *Climate Dynamics*, *43*(11), 2889-2913.http://dx.doi.org/10.1175/BAMS-D-11-00094.1

Vimont DJ, 2011 : Transient Growth of Thermodynamically Coupled Variations in the Tropics under an Equatorially Symmetric Mean State, J. Clim., 23, 5771-5789.

Wade, M., G. Caniaux, Y. DuPenhoat, M. Dengler, H. Giordani, and R. Hummels, 2011 : A one dimensional modeling study of the diurnal cycle in the equatorial Atlantic at the PIRATA buoys during the EGEE-3 campaign. Ocean Dynamics, 61(1), 1-20, doi :10.1007/s10236-010-0337-8.

Wahl, S., M. Latif, W. Park, and N. Keenlyside, 2009 : On the tropical Atlantic SST warm bias in the Kiel climate model, Clim. Dyn., 33(6), 891–906, doi:10.1007/s00382-009-0690-9.

Wang, C., L. Zhang, S.-K. Lee, L. Wu, and C. R. Mechoso, 2014 : A global perspective on CMIP5 climate model biases, Nat. Clim. Change, 4(3) 201–205, doi:10.1038/nclimate2118.

Xie S-P and Philander SGH, 1994 : A coupled ocean-atmosphere model of relevance to the ITCZ in the eastern Pacific Tellus 46A 340-350

Xie, S.-P., 1999: A dynamic ocean–atmosphere model of the tropicalAtlantic decadal variability. J. Climate, 12, 64–70.

Xie S-P and Carton J A, 2004 : Tropical Atlantic variability: Patterns, mechanisms, and impacts. In Earth Climate: The Ocean-Atmosphere Interaction Wang C, Xie S-P and Carton J A (eds.), AGU Geophysical Monograph 147 121-142

Yu, L., X. Jin, and R. A. Weller, 2008: Multidecade Global Flux Datasets from the Objectively Analyzed Air-sea Fluxes (OAFlux) Project: Latent and sensible heat fluxes, ocean evaporation, and related surface meteorological variables. Woods Hole Oceanographic Institution, OAFlux Project Technical Report. OA-2008-01, 64pp. Woods Hole. Massachusetts.